



# Assessment of the electrochemical effects of pulsed electric fields in a biological cell suspension



Djamel Eddine Chafai<sup>a,b</sup>, Andraž Mehle<sup>c</sup>, Amar Tilmatine<sup>b</sup>, Bachir Maouche<sup>a</sup>, Damijan Miklavčič<sup>c,\*</sup>

<sup>a</sup> Département de Génie Électrique, Faculté de Technologie, Université de Bejaia, 06000 Bejaia, Algeria

<sup>b</sup> APELEC Laboratory, Djillali Liabes University of Sidi Bel-Abbes, Sidi Bel-Abbes, Algeria

<sup>c</sup> University of Ljubljana, Faculty of Electrical Engineering, Tržaška 25, SI-1000 Ljubljana, Slovenia

## ARTICLE INFO

### Article history:

Received 12 December 2014

Received in revised form 10 August 2015

Accepted 10 August 2015

Available online 11 August 2015

### Keywords:

Electroporation

Electrochemical impedance spectroscopy

PEF treatment

Cell suspension

Electrode–electrolyte interface

## ABSTRACT

Electroporation of cells is successfully used in biology, biotechnology and medicine. Practical problems still arise in the electroporation of cells in suspension. For example, the determination of cell electroporation is still a demanding and time-consuming task. Electric pulses also cause contamination of the solution by the metal released from the electrodes and create local enhancements of the electric field, leading to the occurrence of electrochemical reactions at the electrode/electrolyte interface. In our study, we investigated the possibility of assessing modifications to the cell environment caused by pulsed electric fields using electrochemical impedance spectroscopy. We designed an experimental protocol to elucidate the mechanism by which a pulsed electric field affects the electrode state in relation to different electrolyte conductivities at the interface. The results show that a pulsed electric field affects electrodes and its degree depends on the electrolyte conductivity. Evolution of the electrochemical reaction rate depends on the initial free charges and those generated by the pulsed electric field. In the presence of biological cells, the initial free charges in the medium are reduced. The electrical current path at low frequency is longer, i.e., conductivity is decreased, even in the presence of increased permeability of the cell membrane created by the pulsed electric field.

© 2015 Elsevier B.V. All rights reserved.

## 1. Introduction

The use of a short and intense pulsed electric field in biotechnology and medicine has led to new methods of cancer treatment, gene therapy, drug delivery and non-thermal inactivation of microorganisms [1, 2,3]. Regardless of the application, the objective is to increase membrane permeability for molecules that cannot otherwise easily cross the cell membrane (electroporation) and hence either facilitate the delivery of foreign materials inside the cell, extract molecules from cell or kill the cell [4]. While the efficiency of the electroporation strongly depends on the pulse parameters, such as pulse amplitude, pulse duration, pulse shape, number of pulses and repetition frequency [5,6], there are many other physical and chemical parameters that affect electroporation efficiency. The multi-scale parameters and their synergy involved in the electroporation make the phenomenon extremely complex and difficult to understand [7]. A number of methods have been used in the study of electroporation based on electrical measurements [8,9,10, 11]. Conductivity measurement has been used in order to determine the variation of membrane conductivity by measuring the instantaneous current and voltage during the pulse application [11]. The nonlinear increase of the conductivity of the cell suspension during the pulse is

attributed principally to the growth of pores created in the first few microseconds of the pulse [12]. Although conductivity measurement is the only way of following up the dynamics of pores (opening and growing), attention needs to be paid to the contribution of the electrochemical impedance of the electrode/electrolyte interface. Electrode/electrolyte interface impedance has strong dispersion of resistance and reactance at low frequencies. Ion diffusion within a double layer of cells also results in low frequency dielectric dispersion [13,14].

On the other hand, when a high-voltage electric pulse is applied to an electrolyte solution, a variety of electrolysis reactions occur at the electrode–solution interfaces in addition to cell membrane permeabilization [15]. Electrolysis occurs when the potential difference is larger than the redox potential of the liquid and the pulse duration is longer than the time taken to charge the electrical double layer. These reactions cause changes in the chemical composition or pH of the experimental medium. Since the pulses applied in electroporation are usually higher than the redox potential, electrolysis occurs [16,17]. The close proximity of the electrodes thus results in contamination of the suspension with electrode material. Moreover, when non-inert electrodes are used, dissolution of the anode material occurs due to oxidation of the metal of the electrode [18]. The rough electrode surface creates local enhancements of the electric field, which lead to inhomogeneity of the electric treatment of each cell and can facilitate the occurrence of electrical breakdown of the liquid samples [19].

\* Corresponding author.

E-mail address: [damijan.miklavcic@fe.uni-lj.si](mailto:damijan.miklavcic@fe.uni-lj.si) (D. Miklavčič).

Electrochemical impedance spectroscopy (EIS), also called the AC impedance method, is a versatile technique for studying the electrical properties of conducting or dielectric materials and their interfaces with electron conducting electrodes. EIS is based on perturbation by a simple AC signal of small amplitude (10 mV to 100 mV) at the steady state of the system under investigation and the response is recorded. Analysis of this response provides system information, such as resistivity, capacitance, diffusion coefficient and double layer capacitance or electron transfer kinetic constants [20]. EIS was therefore used to investigate the final state reached by the electrode–electrolyte–cell system after exposure to a high voltage pulsed electric field, i.e., electroporation pulses.

In this study, we attempt to shed new light on the effects of a pulsed electric field (PEF) during electroporation of a cell suspension. The aim of the study was to evaluate the consequences of PEF on an electrode/electrolyte system free of cells in the first step, whereby a protocol is proposed to distinguish the effects of PEF on the electrodes and on the electrolyte. Since the exposure of cells to a high pulsed electric field leads to membrane permeabilization and involves direct contact between the electrodes and the cells' medium, the cells are expected to be exposed to electrochemical byproducts created at the electrode/electrolyte interface by intermediate electron transfer. In addition, cells were included in the medium and we evaluated the electrochemical phenomena for better understanding the mechanism of the secondary effects of electroporation, other than permeabilization of the cell membrane. Understanding charge transport and the creation of new species in the suspension are of great importance, since this can interfere with membrane electroporation and, especially, the monitoring of cell electroporation.

## 2. Materials and methods

### 2.1. Electrodes, medium and exposure to pulsed electric fields

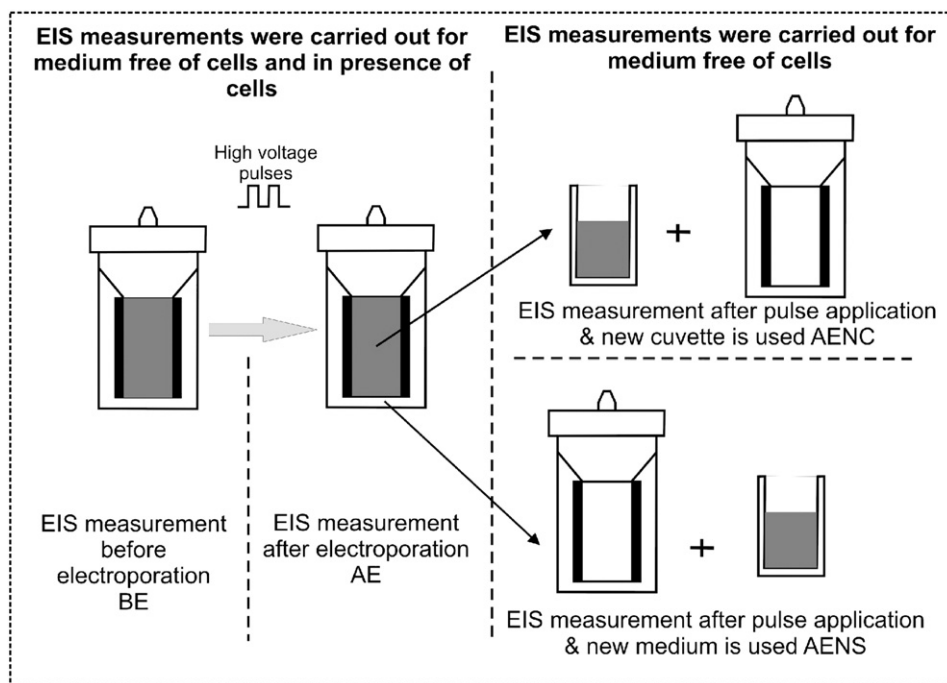
The study was performed using cuvettes with a 2 mm distance between electrodes made of integrated parallel plate aluminum material (Eppendorf, Hamburg, Germany). Electroporation buffers with various

conductivities and composition were used. A 10 mM isosmolar phosphate buffer, designated NaPB ( $\text{Na}_2\text{HPO}_4/\text{NaH}_2\text{PO}_4/\text{MgCl}_2$ , pH = 7.4), [21] of low specific conductivity  $\sigma$  (25 °C) = 0.131 S/m and phosphate buffered saline (PBS) of high specific conductivity  $\sigma$  (25 °C) = 1.365 S/m were used and measured using an MA 5950 conductometer at 1 kHz (METREL, Slovenia). During the experiments, 200  $\mu\text{l}$  of the solution (with or without cells) was placed in the cuvette. A sequence of eight square pulses of 100  $\mu\text{s}$  duration with 1 Hz repetition frequency was applied. Pulse amplitude varied between 60 and 500 V, resulting in an electric field strength of 0.3 kV/cm up to 2.5 kV/cm, estimated by the voltage-to-distance ratio. A laboratory prototype of a Cliniporator (IGEA s.r.l., Carpi, Modena, Italy) was used for pulse generation. During the pulses, the electric current and voltage were measured and stored by a LeCroy oscilloscope (Teledyne LeCroy, Waverunner, LT354M 500 MHz, New York, USA) for postprocessing using a current probe (LeCroy 50 A, New York) and a voltage probe (LeCroy 6 kV, New York). Current variation was calculated in the same manner as used for the total change of conductivity by Pavlin et al. [22]. This variation was defined as the difference between the final conductivity at the end of the eighth pulse and the initial conductivity at the end of the first pulse. The formula is given by:

$$\Delta I\% = (I_8 - I_1)/I_1 \times 100. \quad (1)$$

### 2.2. Protocol and electrochemical impedance measurement

A protocol based on electrochemical impedance spectroscopy (EIS) was used, as depicted in Scheme 1. Electrochemical impedance measurement was performed before (designated BE – before electroporation) and immediately after (designated AE – after electroporation) high voltage/electroporation pulse application (the maximum time between pulse delivery and EIS measurements was 10 s). After applying the pulses, the medium was transferred to a new cuvette and EIS measurement was performed again (designated AENC – after electroporation new cuvette). The previously used cuvette was refilled with new buffer and the EIS measurement was performed (designated AENS –



**Scheme 1.** Presentation of the experimental protocol; EIS measurements were carried out before and after electroporation pulse application in both cases: when the medium was free of cells and in the presence of cells, EIS: electrochemical impedance spectroscopy, BE: before electroporation, AE: after electroporation, AENC: after electroporation new cuvette, AENS: after electroporation new solution.

after electroporation new solution). All measurement results after applying electric pulses were compared to the measurements obtained in the fresh cuvette, i.e., before high voltage electric pulse application.

EIS measurements were carried out using an Agilent HP4284A precision LCR meter controlled by a computer using the LabView interface. Impedance amplitude and phase ( $|Z|$ ,  $\theta$ ) were recorded in the frequency range from 1 MHz to 20 Hz. The experiments were repeated at least three times to ensure reproducibility. Various methods are used to display impedance data. A Bode plot allows direct access to resistances included in the system, whereby the impedance amplitude  $\log |Z|$  and phase  $\theta$  are plotted against frequency  $\log f$ . In a Nyquist plot, the imaginary part of the complex representation of impedance  $Z''$  is plotted against the real part  $Z'$ . This plot allows direct determination of the curve slope due either to Warburg diffusion or surface roughness.

The formula used to calculate the impedance magnitude variation ( $\Delta Z\%$ ) according to the applied electric field is:

$$\Delta Z\% = \left( |Z_x|_{(20 \text{ Hz})} - |Z_x|_{(50 \text{ kHz})} \right) / \left( |Z_{BE}|_{(20 \text{ Hz})} - |Z_{BE}|_{(50 \text{ kHz})} \right) \times 100 \quad (2)$$

where  $Z_x$  is the impedance after pulse application and  $Z_{BE}$  is the impedance before application of electric pulses. The frequency range was from 20 Hz to 20 kHz for NaPB and from 20 Hz to 50 kHz for PBS, whereby the variation was due to electrode polarization. Above 50 kHz, the impedance is constant and depends predominantly on the electrolyte resistance.

### 2.3. Cell preparation

Chinese hamster ovary cells (CHO-K1; European Collection of Cell Cultures, Salisbury, UK) were grown in Ham's F-12 medium (E15-016 without glutamin, PAA Laboratories, Pasching, Austria) supplemented with 10% fetal bovine serum (PAA Laboratories), an antibiotic mix of penicillin/streptomycin (formulation: 50  $\mu$ l of this mix in 500 ml of Ham's medium, with 10,000 units/ml of penicillin, 10 mg/ml of streptomycin in 0.9% NaCl solvent, PAA Laboratories) and 0.05 mg/ml of gentamycin (Sigma-Aldrich, Chemie GmbH, Deisenhofen, Germany), at 37 °C in a humidified 5% CO<sub>2</sub> atmosphere in an incubator (I-CO2-235, Kambič Laboratory Equipment, Slovenia). The cell suspension was obtained by trypsination in 0.25% trypsin/ethylenediaminetetraacetic acid (EDTA, Sigma-Aldrich, Chemie GmbH, Deisenhofen, Germany). The suspension was centrifuged for 5 min (1000 rpm (984  $\times$  g) at 4 °C (Sigma 3K15 centrifuge model, 11133 swing-out rotor for 4 buckets no. 13104, 13177, Germany).

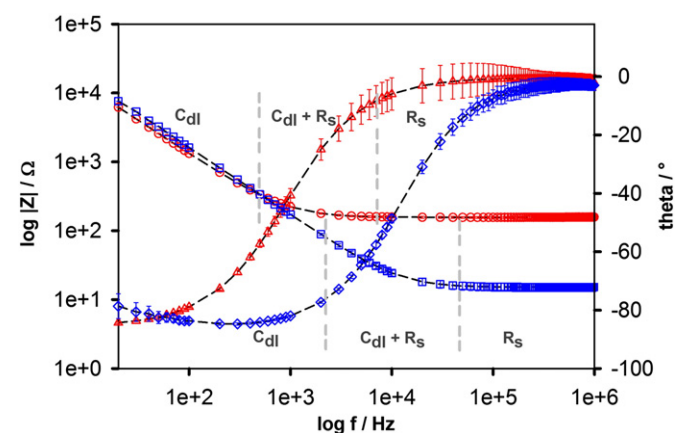


Fig. 1. Average of impedance magnitude and phase measurements shown on a Bode plot before pulse application.  $|Z|$  NaPB ( $\circ$ ),  $\theta$  NaPB ( $\Delta$ ),  $|Z|$  PBS ( $\square$ ),  $\theta$  PBS ( $\diamond$ ).

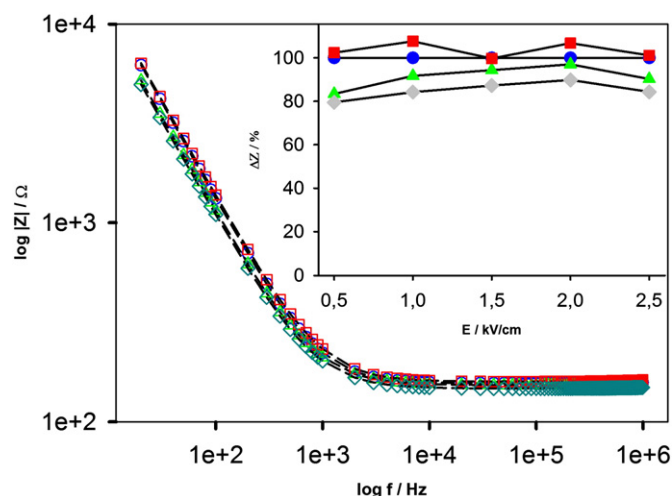


Fig. 2. EIS measurement of the protocol for low conductivity medium NaPB at 0.5 kV/cm. Insert: Impedance variation with respect to the applied electric field. Before electroporation BE ( $\circ$ ), after electroporation AE ( $\Delta$ ), after electroporation new cuvette AENC ( $\square$ ), after electroporation new solution AENS ( $\diamond$ ).

### 2.4. Cell electroporation and propidium iodide uptake

The cell pellet was washed twice with electroporative medium and centrifuged with the same conditions as previously to eliminate all traces of the growth medium [23]. The cell pellet was then resuspended to a final cell density of  $\rho = 1 \times 10^7$  cells/ml in the electroporation medium. The volume of the suspension placed in the cuvette was 200  $\mu$ l for each electric pulse parameter. The same pulse protocol as described in Section 2.1 was used for cell electroporation. Impedance measurements were performed before and after electroporation.

Cell membrane permeabilization was evaluated using a fluorescence dye. Propidium iodide (PI) 2  $\mu$ l of 0.15 mM was added to the suspension immediately before high voltage pulse application. After exposure to high voltage electric pulses, cells were incubated for 3 min at room temperature and then centrifuged for 5 min at 1000 rpm (984  $\times$  g) [24]. The supernatant was removed and 200  $\mu$ l of fresh media was added. Half (100  $\mu$ l) of the suspension was transferred to a 96-multiwell plate for PI uptake evaluation with a spectrophotometer (Tecan infinite M200, Tecan Austria GmbH) at 617 nm. The other half (100  $\mu$ l) of the

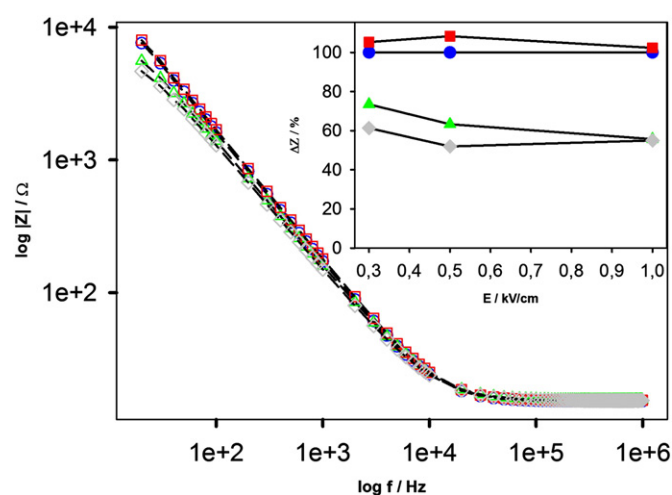
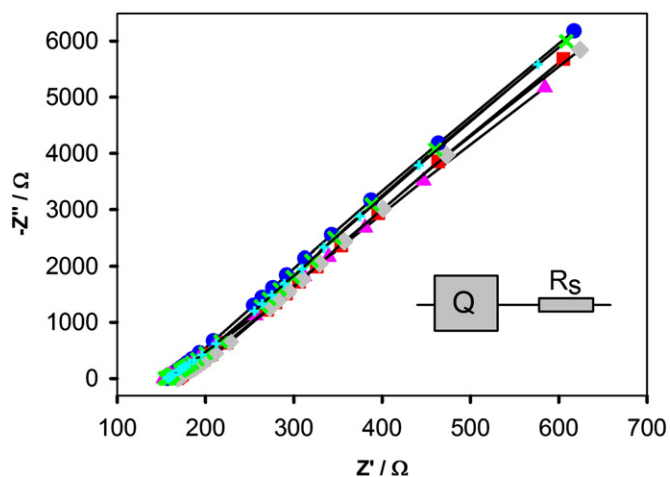


Fig. 3. EIS measurement of the protocol for high conductivity medium PBS at 0.5 kV/cm. Insert: Impedance variation with respect to the applied electric field. Before electroporation BE ( $\circ$ ), after electroporation AE ( $\Delta$ ), after electroporation new cuvette AENC ( $\square$ ), after electroporation new solution AENS ( $\diamond$ ).



**Fig. 4.** Nyquist diagram of low conductivity medium NaPB, Q: constant phase element,  $R_s$ : solution resistance. 0 kV (○), 0.5 kV (Δ), 1 kV (□), 1.5 kV (◇), 2 kV (×), 2.5 kV (+).

suspension was used for the short-term survival test and described in the next paragraph. The PI uptake is defined as:

$$\text{Permeabilization\%} = (F_{(PI,E)} - F_{(PI,E=0)}) / (F_{(PI,max)} - F_{(PI,max)}) \times 100 \quad (3)$$

where  $F_{(PI,E)}$  is the fluorescence intensity of cells for any given pulse intensity,  $F_{(PI,E=0)}$  the fluorescence intensity of cells not exposed to a pulse (negative control) and  $F_{(PI,max)}$  the fluorescence intensity of cells at  $E = 2.5$  kV/cm,  $8 \times 100$  μs, and 1 Hz.

### 2.5. Cell survival

Short-term survival was assessed using propidium iodide (PI) staining. PI fluorescence was measured in a 96-multiwell plate after one hour (1 h) incubation of electroporated cells at 37 °C in a humidified 5% CO<sub>2</sub> atmosphere in the incubator. Cell survival is defined as:

$$\text{Short-term survival\%} = F_{(\text{permeabilization}, E=0)} - F_{(\text{permeabilization}, E)} \quad (4)$$

where  $F_{(\text{permeabilization}, E=0)}$  is considered to be the maximum cell survival, which is equal to 100%, and corresponding to the minimum fluorescence intensity,  $F_{(\text{permeabilization}, E)}$  is the percentage of permeabilized cells for any given pulse intensity.

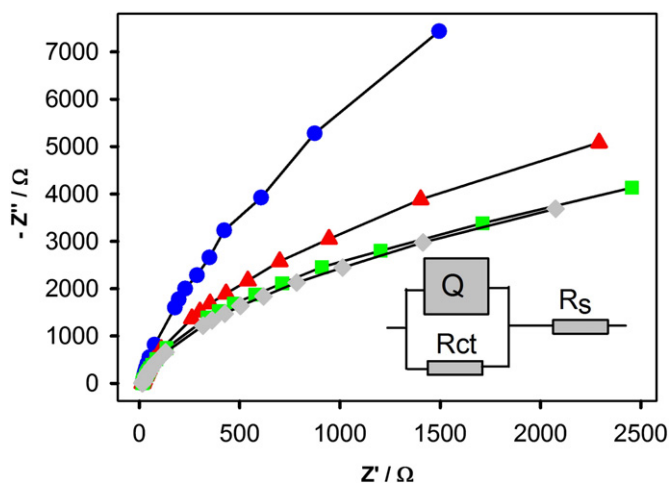


**Fig. 5.** Nyquist diagram of high conductivity medium PBS, Q: constant phase element,  $R_{ct}$ : charge transfer resistance,  $R_s$ : solution resistance. 0 kV (○), 0.3 kV (Δ), 0.5 kV (□), 1 kV (◇).

**Table 1**  
Model parameters for high conductivity medium (PBS).

E (kV/cm)	$R_s/\Omega$	$Q/\Omega^{-1} s^n$	$\alpha$	$R_{ct}/\Omega$
0	15.18	$1.187 \times 10^{-6}$	0.971	$4.321 \times 10^4$
0.3	15.54	$1.6561 \times 10^{-6}$	0.942	$1.643 \times 10^4$
0.5	15.14	$1.713 \times 10^{-6}$	0.933	$1.084 \times 10^4$
1	15.25	$2.134 \times 10^{-6}$	0.92	$1.064 \times 10^4$

$R_s$ : resistance of the solution, Q and  $\alpha$ : constant phase element (CPE) parameters, and  $R_{ct}$ : resistance of charge transfer.

Long-term survival was assessed using an MTS assay (CellTiter 96® AQueous One Solution Cell Proliferation Assay, Promega Corporation, USA). Survival was determined 48 h after electroporation using the same protocol as described above. Cells were prepared in a 96-multiwell plate containing a final volume of 100 μl/well with  $1 \times 10^4$  cells/ml final density.

Twenty microliters of MTS solution was added to each well and incubated for 3 h at 37 °C. Absorbance was recorded at 490 nm using a Tecan spectrophotometer [25]. Cell survival is defined as:

$$\text{Long-term survival\%} = (F_{(E)} - F_{(BG)}) / (F_{(E=0)} - F_{(BG)}) \times 100 \quad (5)$$

where  $F_{(E)}$  is the absorbance intensity of cells for any given pulse intensity,  $F_{(BG)}$  the background absorbance intensity (culture medium) and  $F_{(E=0)}$  the absorbance intensity of cells at  $E = 0$  kV/cm.

## 3. Results and discussion

Impedance spectroscopy measurements were performed to study electrochemical phenomena (electrochemical reactions, interface phenomenon and electrode alteration) during cell electroporation. The investigation was performed in two steps. In the first step, we explored the effects of the pulsed electric field in a medium free of cells (electrode/electrolyte system), thus to assess the existence and probable contribution of electrochemical phenomena to the cell electroporation mechanism. In the second step, cells were added to the medium and a re-assessment of electrochemical phenomena was performed (electrode/electrolyte/cells system).

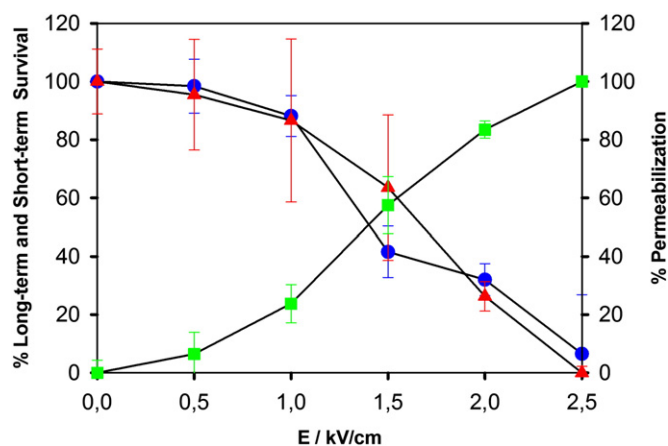
### 3.1. Electrode/electrolyte interface

Fig. 1 shows the average of impedance magnitude and phase measurements shown on the Bode plot before high voltage electric pulse application, in media of various conductivities without cells in the whole frequency domain from 20 Hz to 1 MHz. The impedance magnitude spectrum shows the presence of three frequency dependent regions. A negative slope due to the double layer capacitance  $C_{dl}$  behavior of the electrode/electrolyte interface is dominant from 20 Hz to 200 Hz and from 20 Hz to 1.5 kHz for NaPB and PBS, respectively. There is then a bend, at which both double layer capacitance and electrolyte resistance are present ( $R_s, C_{dl}$ ), from 200 Hz to 20 kHz and 1.5 kHz to 50 kHz for NaPB and PBS, respectively. The third region is a plateau dominated by the resistance of the solution  $R_s$ . In return, the phase spectrum shows

**Table 2**  
Model parameters for low conductivity medium (NaPB).

E (kV/cm)	$R_s/\Omega$	$Q/\Omega^{-1} s^n$	$\alpha$	$R_{ct}/\Omega$
0	153.6	$1.594 \times 10^{-6}$	0.9516	$1.27 \times 10^6$
0.5	167	$1.833 \times 10^{-6}$	0.945	$1.209 \times 10^{13}$
1	167	$1.833 \times 10^{-6}$	0.945	$1.209 \times 10^{13}$
1.5	169	$1.781 \times 10^{-6}$	0.9456	$4.643 \times 10^{13}$
2	156.1	$1.746 \times 10^{-6}$	0.9455	$3.155 \times 10^{14}$
2.5	157	$1.862 \times 10^{-6}$	0.9458	$7.736 \times 10^{13}$

$R_s$ : resistance of the solution, Q and  $\alpha$ : constant phase element (CPE) parameters, and  $R_{ct}$ : resistance of charge transfer.



**Fig. 6.** Permeabilization, long-term and short-term survival, data point present average of at least 5 experiments, vertical bars represent standard deviation. Long-term survival (○), short-term survival (△), permeabilization (□).

the same regions of behavior, whereby the spectrum starts from around  $90^\circ$ , which is typical capacitive and decreases to  $0^\circ$ , which is typical resistive, as shown in Fig. 1 for NaPB and PBS media, respectively.

It is important to note that the high conductivity medium impedance (PBS) is 18% higher than the low conductive medium impedance (NaPB) at the low frequency range from 20 Hz to 100 Hz. However, at high frequency (plateau region representing solution resistance), the impedance of NaPB is 10 times higher than PBS, which is in agreement with the conductivity values of the solutions (conductivity of PBS at  $25^\circ\text{C}$  is 10 times higher than with NaPB). This phenomenon is probably due to the free movement/orientation of electrolyte ions, which leads to high polarization since the molecules can follow the low frequency in the high conductive medium. However, this observation is only valid before pulse application. After pulse application, the phenomenon is no longer noticeable, which is probably a consequence of an ionic balance change.

Experimental data extracted from EIS measurements of the protocol proposed and described in Section 2 (Materials and methods) are plotted in Fig. 2 and Fig. 3 for low conductivity (NaPB) and high conductivity (PBS) media, respectively, for a 2 mm gap between electrodes. The applied electric field for PBS was limited to 1 kV/cm because of the generator maximum current limitation. The results show that the impedance after pulse application of the solution transferred to the new cuvette (AENC) is roughly the same as before pulse application (BE). On the other hand, the impedance of the cuvette exposed to electric pulses and filled with fresh solution (AENS) is roughly the same as after pulse application (AE), meaning that changes are predominantly occurring at the electrode interface. The results of experiments performed

with 1 mm and 4 mm electrode gaps were similar (data not reported). Reuse of cuvettes is not therefore recommended.

The internal resistance of the electrode/electrolyte system is the sum of both electronic and ionic resistance contributions. The ionic contribution is due to the electrolyte resistance located in the space between the electrodes, and conductivity is ensured by ionic charges. The electronic resistance is the intrinsic electronic resistivity of the electrode material. The intrinsic electronic conductivity of the electrode is too high (e.g., metal) and ensured by electronic charges, hence, has a minor contribution to the internal resistance of the system. The conductivity difference between the two phases (electrode/electrolyte) thus leads to charge accumulation at the interface. This accumulation of charge at the interface creates what is called a double layer of opposite signs, depending on the potential applied to the electrode [26]. The electrodes are the site of redox reaction processes governing electronic transfer from one phase to another through the interface. The charge transfer is more or less moderate/fast, depending on the interface structure.

The goal of the proposed protocol was to distinguish the effects of the pulsed electric field on the electrode/electrolyte interface. This allows an understanding of the electrochemical mechanism caused by the pulsed electric field. The initial hypothesis was that when both the electrode and electrolyte are exposed to electric pulses together, designated AE, a pulsed electric field causes changes to both parts. Afterwards, the pulsed electrode/electrolyte interface was separated and recreated as two new interfaces, designated AENC and AENS, each with the thumbprint of the applied pulsed electric field. The impedance measurement of AENC showed a return to the initial values, with a deviation of less than 10% higher compared to before pulsing (BE); the thumbprint of the high voltage electric field on the solution was hence lost. If the pulsed electric field had a direct influence on the solution by creating new charged species, these are therefore neutralized or diffuse. On the other hand, the measurement of AENS showed a return to initial values, with a deviation of approximately 10% lower than in the case of after pulsing (AE); the thumbprint of the electric field on the electrode was thus retained, even without a second exposure to the pulsed electric field. The new interface with the new solution therefore depends on the state of the electrode surface. The electrode surface change is more prominent in the case of a non-inert metal electrode, such as aluminum, which releases metal ions into the solution under primary anodic half reactions ( $2\text{Al (solid)} \rightarrow 2\text{Al}^{3+} \text{ (aq)} + 6\text{e}^-$ ) [27]. The protocol results show that the main effect of the pulsed electric field at the electrode/electrolyte interface is due to an electrode surface state modification.

### 3.2. Electrochemical reactions

On the same figures (Figs. 2 and 3), the impedance variation with respect to the electric field is shown as an inset. It is important to note that

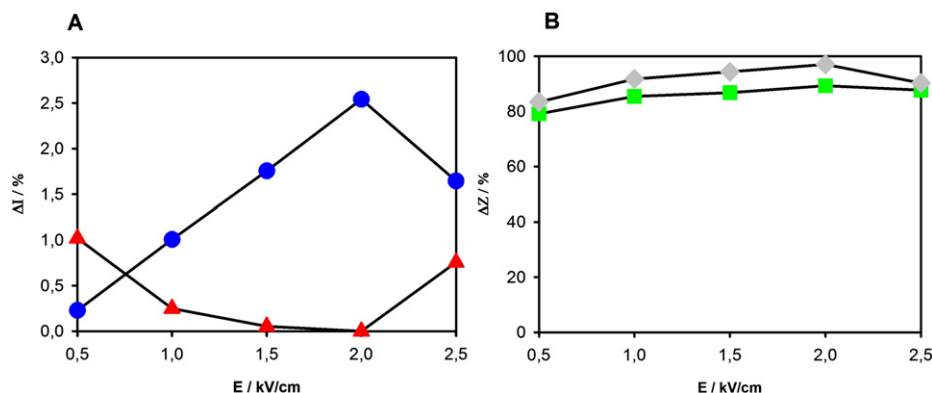


**Fig. 7.** Total current variation during electroporation (a) and impedance variation measured immediately after electroporation (b) of the suspension with and without cells, I<sub>c</sub>: current of cell suspension (○), I<sub>s</sub>: current of the solution without cells (△), Z<sub>c</sub>: impedance of cell suspension (□), Z<sub>s</sub>: impedance of solution without cells (◇).

electrochemical processes are cumulative and species created by redox reactions accumulate pulse after pulse. Since the difference in conductivity between the electrode and the high conductive medium (PBS) is not large, the accumulation is low at the interface and current flows readily through the medium and the injected charge is accommodated by these reactions. However, in the case of the low conductive medium,

a large amount of the injected charge is accommodated on the double layer prior to initiating faradaic reactions. It is important to note that impedance measurements were done immediately after pulse application to assess the electrochemical phenomena produced by the pulsed electric field, in addition to those induced by the conventional electrolyte/electrode interface created by a low AC current. Figs. 2 and 3 show the

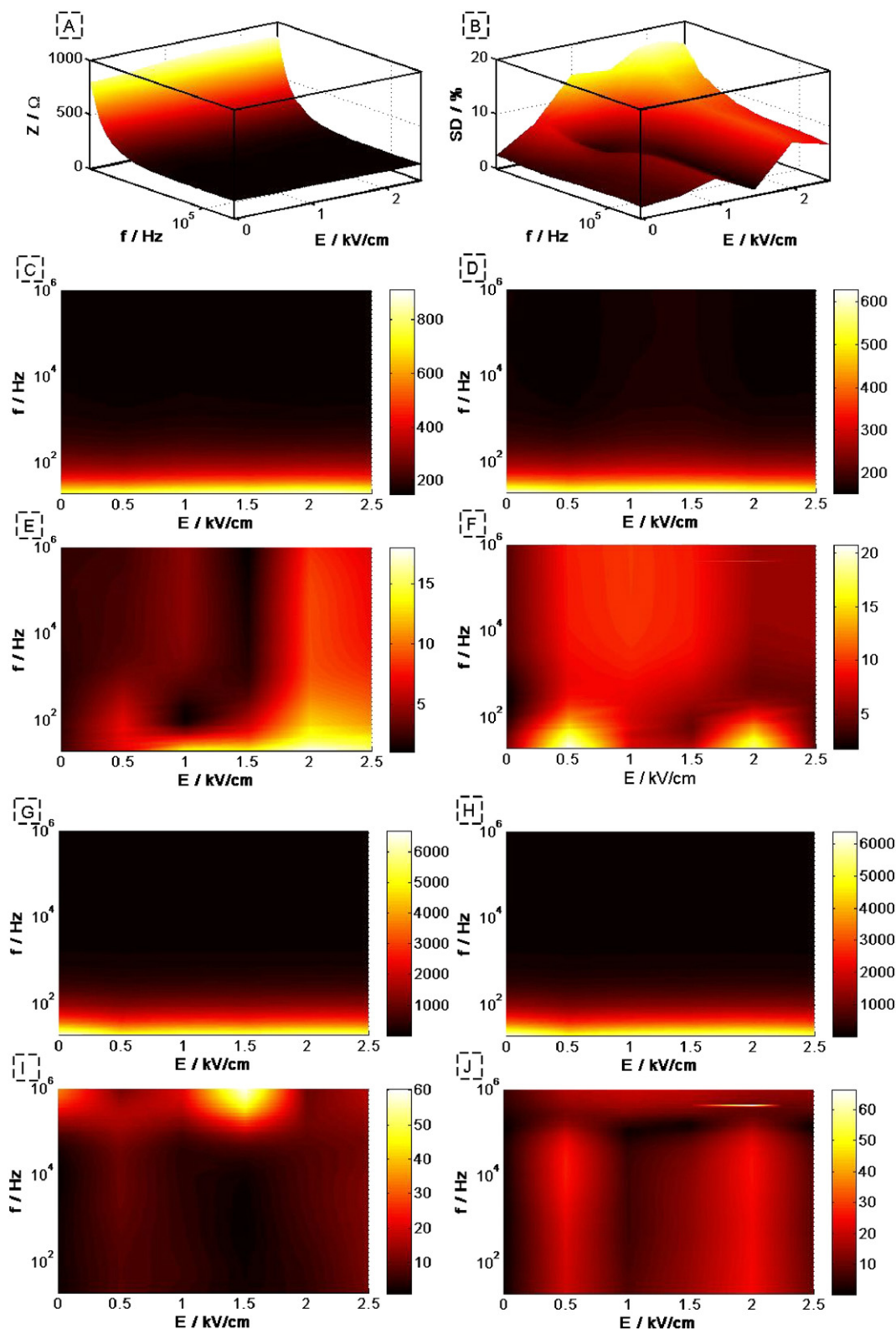


**Fig. 8.** Resistance and reactance of medium without cells and cell suspension. (A and B) resistance and standard deviation (SD) of the cell suspension in 3D, (C and E) resistance and SD of cell suspension, (D and F) resistance and SD of solution, (G and I) reactance and SD of cell suspension, (H and J) reactance and SD of solution.

dependence of the electrode/electrolyte interface on the electric field and the electrolyte conductivity.

In the case of the low conductivity medium up to 2 kV/cm, a small amount of the injected charge changes the conductivity at the interface, which is observed as a reduction of the impedance, and since those charges cannot diffuse because of the high resistivity of the medium, they accumulate at the interface. This charge accumulation forms the interfacial capacitance and increases the impedance until reaching the initial impedance before pulse application. Aluminum passivation is another process that leads to the creation of this interfacial capacitance and is more related to anodic reactions. In the case of the high conductivity medium (Fig. 3), the injected charge is not accumulated at the interface. Bubbles and turbulent flow were violently generated and promoted the spread of ions generated during electrolysis throughout the whole solution, as reported by Kim et al. [28]. Principally, primary reactions lead to electrode dissolution and secondary reactions lead to hydrogen evolution in the solution generated at the interface during primary reactions. Both of these reactions have a non-uniform density charge distribution and occur separately at the anode and the cathode, which potentially hinders the uniform electric field.

### 3.3. Surface alteration and electrode dissolution due to a high intensity pulsed electric field

The parameters of the electrode/electrolyte interface were evaluated by fitting the experimental data to an equivalent electrical model that describes the above discussed electrochemical processes, as shown in Fig. 5. The equivalent electrical model depends on the structure of the interface, which is strongly related to the electrode surface and medium conductivity. Figs. 4 and 5 show the Nyquist diagram, which represents the imaginary part of the impedance versus the real part for various electric field intensities of NaPB and PBS, respectively. The figures clearly show a non-ideal capacitive behavior of the interface before pulse application, i.e., 0 kV/cm, in both low (NaPB) and high (PBS) conductivity solutions, which leads to constant phase element (CPE) behavior. CPE behavior can be explained in general by surface roughness and heterogeneities, electrode porosity, variation of the coating composition, slow adsorption reactions and non-uniform potential and current distribution [29]. The NaPB plot shows typical constant phase element behavior, which is a straight line before and after pulse application. In contrast, the PBS plot shows a significant influence of the pulsed electric field applied to the interface.

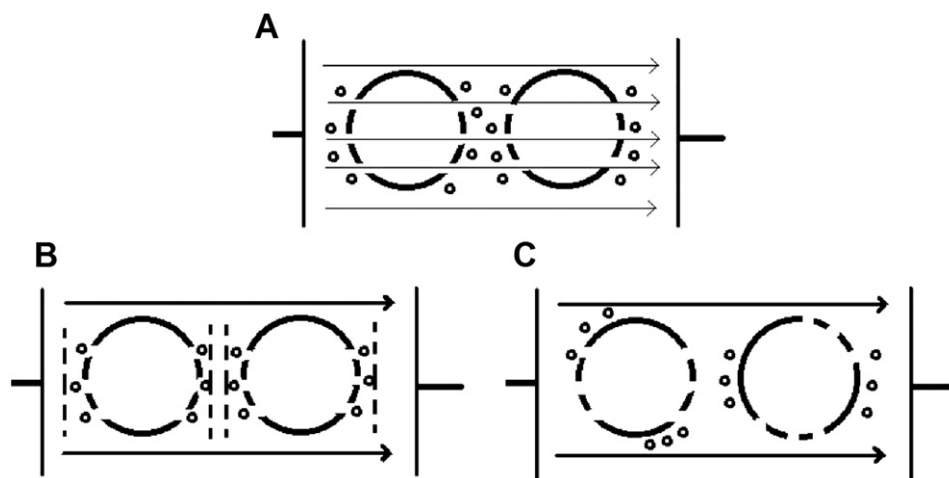
The model used for data fitting is based on the constant phase element (CPE) of parameters ( $Q$ ,  $\alpha$ ) in parallel with the resistance of

charge transfer ( $R_{ct}$ ), and in series with the resistance of the solution ( $R_s$ ). The parameters  $R_s$ ,  $Q$ ,  $n$  and  $R_{ct}$  determined for each set of experimental data are shown in Table 1 for the high conductive medium (PBS) and in Table 2 for the low conductive medium (NaPB).

An increase in the electric field intensity is accompanied by an increase in  $Q$  and a decrease in  $\alpha$  and  $R_{ct}$  in the case of PBS after pulse application. The increase in the  $Q$  capacitive parameter is related to the presence of more charged species generated by the pulsed electric field. On the other hand, the decrease in the  $R_{ct}$  parameter is related to the increase in the rate of chemical reactions. In the case of NaPB, the parameters  $Q$  and  $\alpha$  are roughly uniform. In contrast,  $R_{ct}$  has a high value after pulse application, of the order of  $10^{13}$ , compared to the value before pulse application, which is in the order of  $10^6$ ; the initial model can thus be reduced to a model of a blocked electrode with a CPE capacitance in series with  $R_s$ .

It is important to note that the  $R_s$  of the low conductive medium is affected by the pulsed electric field. This phenomenon was already mentioned in the above discussion of the protocol. Since the charge is accumulated on the interface and transferred by irreversible electrochemical reactions to the medium during the application of high voltage electric pulses, an accumulated charge presence is detected by the EIS measurements, leading to an increase in the impedance.

To summarize, the EIS impedance investigation into the effects of a pulsed electric field under the same conditions as used in cell electroporation shows a significant contribution of electrochemical phenomena to modification of the cell environment. These modifications principally affect the electrodes, in both cases of the electrode/electrolyte (high conductive or low conductivity electrolyte) interface. Surface roughness and non-uniform potential and current distribution are highly pronounced, as already described by Saulis et al. [19]. A significant modification of the electrolyte resistance was observed in the low conductivity medium, caused by accumulated charges in the double layer and released to the medium across the interface. The pulsed electric field also has an influence on the bend and plateau regions of the impedance spectrum. The low conductivity medium interface with the electrode presents two principal phenomena (alteration of electrode and high charge accumulation) that may interfere with cell electroporation. In addition to the effects cited for the low conductivity medium, a high conductivity medium produces other interfering phenomena, such as heating [30]. For this reason, cells in low conductive medium were studied using the same procedure to assess only the contribution of electrochemical phenomena in the electroporation process, and are discussed in the following sections.



**Scheme 2.** (A) EIS current path after electroporation through the pores created on the membrane, (B) and (C) when the current path is modified due to new interfaces created (B) and cell rotation (C).

### 3.4. Cell membrane permeabilization and cell survival

Fig. 6 shows PI uptake in CHO cells indicative of membrane permeabilization and short-term and long-term survival assessed by the addition of PI immediately before treatment and by the MTT test, respectively, as a function of the electric field. The short-term survival and long-term survival are approximately the same, so no significant contribution of probable toxic material release from the electrodes on the time scale of viability tested was detected. This may be due to the high resistivity (i.e., low conductivity) of the medium, which does not lead to a high rate of electrochemical reactions and diffusion in low conductivity medium, as already discussed in the previous part of the Results and discussion section but, in contrast, leads to high electric field inhomogeneity.

### 3.5. Electric current variation and impedance variation of cell suspension

Fig. 7A shows the variation of current measured during cell electroporation and during application of electric pulses in the absence of cells. Impedance variation measured immediately after electroporation of the medium without cells and the cell suspension also is shown in Fig. 7B.

In Fig. 7A, the total cell suspension current variation calculated according to Eq. (1) (designated  $\Delta I_C$ ) increases to a maximum value with an increase of the electric field up to 2 kV/cm, while the total solution (free of cells) current variation (designated  $\Delta I_S$ ) decreases to a minimum value at the same amplitude of electric field as in the cell suspension current. It is important to note that these currents were measured during PEF application in the case of both the cell suspension and the solution without cells. However, the impedance was measured immediately after pulse application. In this case, impedance results describe the bioelectrochemical phenomena after electric pulse delivery using very low voltage. The solution (free of cells) impedance variation (designated  $\Delta Z_S$ ) calculated according to Eq. (2) shows a minimum drop of impedance after pulse delivery, to the initial values before the delivery of pulses. The minimum current variation of the solution is thus explained by accumulative behavior (i.e., more charges are produced due to the electric field, fewer are dissipated by electrochemical reactions because of the high resistivity of the medium) at the interface. In other words, the current difference during delivery/application of pulses to the suspension without cells between the first and the eighth pulse is constant up to 2 kV/cm. This result is very important because it shows that there is a threshold at which the electrode/electrolyte interface was apparently breached.

In the case of the cell suspension, the impedance measured after electroporation decreased compared to the values before electroporation, which corresponds to the ion efflux from the cell interior (note that cells are diluted/bathed in the low conductivity medium). However, with a low electric field, the 0.5 kV/cm level corresponds to less than 10% of the PI uptake, and the cell suspension impedance variation (designated  $\Delta Z_C$ ) drops to maximum values, which does not reflect the conductivity changes due to the minimum cell ion efflux. There was thus interference of the electrochemical phenomena during current measurements. A similar observation was already made by Ramos and Heric [14]. Since the cell interior is released to the medium, new interfaces are created, on the one hand by the closest cells to the electrodes and, on the other, between cells that are originally subject to an inhomogeneous local electric field. These interfaces are created between every adjacent pore, forming a pore/medium/pore interface on two different cells and randomly distributed, which apparently increases the total impedance of the cell suspension. At the same threshold, in the conditions of our study, 2 kV/cm, the variation in the cell suspension current was maximum and impedance dropped to the minimum value (the electrode/electrolyte interface of the solution free of cells was suppressed). We consider this threshold to be important, at which ion efflux due to pore creation is maximum and represents the real efflux due to electroporation without electrochemical interference.

### 3.6. Electrochemical and interfacial phenomena in the presence of cells

Fig. 8 shows the resistance and reactance and the corresponding standard deviation for the cell suspension and for the medium without cells. The representation is in 3D, according to the frequency, amplitude (impedance or standard deviation) and electric field as shown for the cell suspension (resistance in Fig. 8A and standard deviation in Fig. 8B) and then a projection on the X–Y axis is given. The resistance of the cell suspension (Fig. 8C) is higher than the medium resistance without cells (Fig. 8D) at low frequency. Scheme 2A shows the expected current path through the pores created on the membrane but the increase of the real part may be a consequence of new interfaces (capacitances) created after electroporation, as shown in Scheme 2B, probably due to the diffusion kinetics mechanism of the charges, or the rotation of cells or migration of charges resulting in an apparent rotation of cells (Scheme 2C), which also modifies the current path. It is important to note that the low conductivity of the medium does not allow diffusion of free charges. This observation has already been reported in the case of an intact cell membrane by Ø.G. Martinsen et al. [31]. The standard deviation (SD) of the resistance of the medium without cells (Fig. 8F) shows a dispersion of results at 0.5 kV/cm and 2 kV/cm at low frequency, corresponding to the maximum and minimum values of solution current variation mentioned previously, which may be caused by the dispersed values of the inhomogeneous distribution of current at the interface. The resistance standard deviation of the cell suspension (Fig. 8E) is high at high voltage, at which the current variation was maximum (all intracellular ions are released to the medium), and may be caused by the polarization of permeabilized cells, which can be randomly oriented. The resistance SD is more pronounced in the range of 2 kV/cm to 2.5 kV/cm, even for higher frequencies, where small free charges (ions) can probably follow the frequency and the current takes different paths through the random position of the electroporated cells. In contrast, the reactance of the medium free of cells and the reactance of the cell suspension (Fig. 8H and G, respectively) are roughly the same, as are standard deviations (Fig. 8J and I, respectively), except at high frequency. The reactance is therefore mainly due to the electrode/electrolyte interface.

## 4. Conclusions

We obtained experimental data using electrochemical impedance spectroscopy (EIS), quantitatively characterizing electrochemical phenomena related to the electroporation process in a cell suspension. EIS was used to identify the effects of a pulsed electric field in medium free of cells, as well as in cell suspension. Impedance spectroscopy uses a very low voltage to assess the final state reached after electroporation and to confirm the existence of secondary effects of a pulsed electric field such as electrochemical phenomena, other than cell membrane electroporation. New insight was obtained into the kinetics of diffusion due to the creation of new interfaces at low frequency, which leads to a current path increase, i.e., decreased conductivity even with the presence of membrane pores.

## Acknowledgments

The presented work was supported by the Slovenian Research Agency (P2-0249 and IP-0510), APELEC Laboratory, and University of Bejaia (CNEPRU N°A01L07UN220120140037) and was possible due to the networking effort of COST TD 1104 Action (<http://www.electroporation.net>). D.E.C. was the recipient of STSM grant no. TD1104-14254. D.E.C. would like to thank Duša Hodžić, Saša Haberl and Matej Reberšek for their guidance when he began working in the Biocybernetics Laboratory at the Faculty of Electrical Engineering, University of Ljubljana.

## References

- [1] S. Haberl, D. Miklavčič, G. Serša, W. Frey, B. Rubinsky, Cell membrane electroporation – part 2: the applications, *IEEE Electr. Insul. M.* 29 (1) (2013) 29–37.
- [2] S. Mahnič-Kalamiza, E. Vorobiev, D. Miklavčič, Electroporation in food processing and biorefinery, *J. Membr. Biol.* 247 (2014) 1279–1304.
- [3] M.L. Yarmush, A. Golberg, G. Serša, T. Kotnik, D. Miklavčič, Electroporation-based technologies for medicine: principles, applications, and challenges, *Annu. Rev. Biomed. Eng.* 16 (2014) 295–320.
- [4] T. Kotnik, P. Kramar, G. Pucihar, D. Miklavčič, M. Tarek, Cell membrane electroporation – part 1: the phenomenon, *IEEE Electr. Insul. M.* 28 (5) (2012) 14–23.
- [5] T. Kotnik, G. Pucihar, M. Reberšek, D. Miklavčič, L.M. Mir, Role of pulse shape in cell membrane electroporation, *Biochim. Biophys. Acta* 1614 (2003) 193–200.
- [6] G. Pucihar, D. Miklavčič, L.M. Mir, The effect of pulse repetition frequency on the uptake into electroporated cells in vitro with possible application in electrotherapy, *Bioelectrochemistry* 57 (2002) 167–172.
- [7] E. Neumann, Membrane electroporation and direct gene transfer, *Bioelectrochem. Bioenerg.* 28 (1992) 247–267.
- [8] A. Ivorra, B. Al-Sakere, B. Rubinsky, L.M. Mir, *In vivo* electrical conductivity measurements during and after tumor electroporation: conductivity changes reflect the treatment outcome, *Phys. Med. Biol.* 54 (2009) 5949–5963.
- [9] M. Kranjc, F. Bajd, I. Serša, D. Miklavčič, Magnetic resonance electrical impedance tomography for measuring electrical conductivity during electroporation, *Physiol. Meas.* 35 (2014) 985–996.
- [10] R.V. Davalos, D.M. Otten, L.M. Mir, B. Rubinsky, Electrical impedance tomography for imaging tissue electroporation, *IEEE Trans. Biomed. Eng.* 51 (5) (2004) 761–767.
- [11] D. Cukjati, D. Batiuskaite, F. André, D. Miklavčič, L.M. Mir, Real time electroporation control for accurate and safe *in vivo* non-viral gene therapy, *Bioelectrochemistry* 70 (2007) 501–507.
- [12] M.E. Mezeme, G. Pucihar, M. Pavlin, C. Brosseau, D. Miklavčič, A numerical analysis of multicellular environment for modeling tissue electroporation, *Appl. Phys. Lett.* 100 (2012) 143701.
- [13] A. Ramos, A.L.S. Schneider, D.O.H. Suzuki, J.L.B. Marques, Sinusoidal signal analysis of electroporation in biological cells, *IEEE Trans. Biomed. Eng.* 59 (10) (October 2012).
- [14] A. Ramos, F.D. Heric, Numerical analysis of impedance spectra of yeast suspensions, *Journal of Microwaves, Optoelectronics and Electromagnetic Applications* 12 (2) (December 2013).
- [15] A. Silve, J. Villemejeane, V. Joubert, A. Ivorra, L. Mir, Nanosecond pulsed electric field delivery to biological samples: difficulties and potential solutions, *Advanced Electroporation Techniques in Biology and Medicine*, CRC Press, 2010.
- [16] R. Rodaite-Riseviciene, R. Saule, V. Snitka, G. Saulis, Release of iron ions from the stainless-steel anode occurring during high-voltage pulses and its consequences for cell electroporation technology, *IEEE Trans. Plasma Sci.* 42 (2014) 249–254.
- [17] J.T. Fleming, Electronic interfacing with living cells, *Whole Cell Sensing Systems I, Advances in Biochemical Engineering/Biotechnology*, vol. 117 2010, pp. 155–178.
- [18] T. Kotnik, D. Miklavčič, L.M. Mir, Cell membrane electroporation by symmetrical bipolar rectangular pulses. Part II. Reduced electrolytic contamination, *Bioelectrochemistry* 54 (2001) 91–95.
- [19] G. Saulis, R. Rodaite-Riseviciene, V. Snitka, Increase of the roughness of the stainless-steel anode surface due to the exposure to high-voltage electric pulses as revealed by atomic force microscopy, *Bioelectrochemistry* 70 (2007) 519–523.
- [20] J.R. Macdonald, Impedance spectroscopy, *Ann. Biomed. Eng.* 20 (1992) 289–305.
- [21] I. Marjanovic, S. Haberl, D. Miklavčič, M. Kanduser, M. Pavlin, Analysis and comparison of electrical pulse parameters for gene electrotransfer of two different cell lines, *J. Membr. Biol.* 236 (2010) 97–105, <http://dx.doi.org/10.1007/s00232-010-9282-1>.
- [22] M. Pavlin, M. Kanduser, M. Reberšek, G. Pucihar, F.X. Hart, R. Magjarevic, D. Miklavčič, Effect of cell electroporation on the conductivity of a cell suspension, *Biophys. J.* 88 (June 2005) 4378–4390.
- [23] G. Pucihar, T. Kotnik, M. Kanduser, D. Miklavčič, The influence of medium conductivity on electroporation and survival of cells in vitro, *Bioelectrochemistry* 54 (2001) 107–115.
- [24] S. Haberl, D. Miklavčič, M. Pavlin, Effect of Mg ions on efficiency of gene electrotransfer and on cell electroporation, *Bioelectrochemistry* 79 (2010) 265–271.
- [25] T.L. Riss, R.A. Moravec, A.L. Niles, H.A. Benink, T.J. Worzella, L. Minor, *Cell Viability Assays, Assay Guidance Manual*, Eli Lilly & Company and the National Center for Advancing Translational Sciences, 2004.
- [26] E.T. McAdams, A. Lackermeier, J.A. McLaughlin, D. Macken, The linear and non-linear electrical properties of the electrode–electrolyte interface, *Biosens. Bioelectron.* 10 (1995) 67–74.
- [27] G. Saulis, Electrochemical processes occurring during cell electromanipulation procedures. A short review, in: *Electroporation in Laboratory and Clinical Investigations*, E.P. Spugnini, A. Baldi (Eds.), pp. 99–113, Nova Science Publishers, Inc., Hauppauge, NY, USA, 2012.
- [28] J.A. Kim, K. Cho, M.S. Shin, W.G. Lee, N. Jung, C. Chung, J.K. Chang, A novel electroporation method using a capillary and wire type electrode, *Biosens. Bioelectron.* 23 (2008) 1353–1360.
- [29] J.B. Jorcin, M.E. Orazem, N. Pèbère, B. Tribollet, CPE analysis by local electrochemical impedance spectroscopy, *Electrochim. Acta* 51 (2006) 1473–1479.
- [30] D. Miklavčič, M. Puc, *Electroporation*, Wiley Encyclopedia of Biomedical Engineering, John Wiley & Sons, Inc., 2006.
- [31] Ø.G. Martinsen, S. Grimnes, H.P. Schwan, Interface phenomena and dielectric properties of biological tissue, *Encyclopedia of Surface and Colloidal Science*, 2002.